Intl. J. River Basin Management Vol. 5, No. 4 (2007), pp. 253–265

Development of an unsteady model for flow through coarse heterogeneous porous media applicable to valley fills

S.M. HOSSEINI, *Associate Professor, Civil Engineering Department, Ferdowsi University of Mashhad, Mashhad, Iran, P.O. Box 91775-1111*

D.M. JOY, *Associate Professor, School of Engineering, University of Guelph, Guelph, Ontario, Canada, N1G 2W1*

ABSTRACT
A one-dimensional numerical model, ROCKFLOW, has been developed to analyze unsteady non-linear flow through coarse porous media. The model is particularly applicable to flow through valley fills and rock drains resulting from mining operations and takes factors such as the spatial variability of material properties and the variability of the cross-sectional geometry into account. The modified Saint-Venant equations together with the Forchheimer equation constitute the mathematical formulation of the flow system. The model employs a four-point finite difference method and a Newton-Raphson scheme to solve the resulting non-linear equations. With regard to the vertical heterogeneity of the materials, a superposition method has been developed and used in the model to account for changes in material properties. Laboratory studies on three, 1.5 m long, rockfills made of different homogeneous materials and also a layered rockfill were used to verify the model under different initial and boundary conditions. First, the material hydraulic parameters were determined using steady-state conditions in the physical models. The resulting hydraulic parameters were then used to model unsteady conditions. It was found that the model is able to reproduce the experimental results well in terms of both water surface profiles and depth variation with time curves in the physical models. There is a need to minimize the environmental impacts of mining activities. ROCKFLOW can be applied to valley fills under field conditions to test various design scenarios and to thereby assess their potential impact on the environment (e.g. modified flow regime in the downstream channel).

Keywords: Coarse porous media; gradually-varied flow; rockfill; unsteady flow; valley fill.

1 Introduction

Mining activities can be a serious source of environmental concerns, considering the amount of waste that they may create. Aubertin *et al.* (1996) and Greenly and Joy (1996) provide good examples of the amount of waste that may be generated from mining activities. One method of waste rock disposal is to use a technique known as a valley fill (Cowherd, 1981; Findikakis and Tu, 1985). This involves placing waste rock in stream valleys close to mining sites. Such dumps may be several kilometers long and composed of a wide range of material sizes. These dumps in some areas may act as dams which retain flood waves during intense storms and water depths of 40 m have been observed in the temporary reservoirs upstream of such dumps (Findikakis and Tu, 1985).

There are also environmental concerns about such facilities. These concerns are mainly due to the acid and sediment generated from the dumps that may affect water quality and disturb the aquatic life in receiving streams (Joy, 1990; Cowherd, 1981). At present there are not adequate analytical tools to reasonably predict the acid and sediment production from these installations. Understanding the flow behavior inside these structures is the first step for determination of the potential acid and sediment generation.

A common characteristic of rockfill structures including valley fills is that flow through this porous media often deviates from Darcy's law and a non-linear flow equation is required. The occurrence of unsteady, free-surface flow serves to increase the complexity of flow through valley fills. Spatial and temporal variability of materials further complicates the prediction of flow through valley fills. When rock is dumped from a height, as is typically done for these installations, the larger materials naturally roll to the bottom with progressively smaller materials remaining near the top and therefore a segregated fill is created. This naturally creates a large drainage blanket over the entire bottom of the valley (Cowherd, 1981).

In this study, a model, ROCKFLOW has been developed to model the hydraulic flow behavior in structures such as valley fills. This has been done while considering the key characteristics of valley fills such as the unsteadiness of flow, heterogeneity in material properties and variability in slope and cross section of the valley fill. In order to verify the applicability of the ROCKFLOW model to rockfill and the accuracy of the model outputs, experiments were conducted in laboratory to collect necessary data. The experiments were done in a laboratory flume available at the School of Engineering, University of Guelph. Three rectangular rockfill structures made of homogeneous materials with different sizes were constructed in the flume. The fourth rockfill structure was a layered system to study the effect of segregation on the flow behavior. Different steady discharges and hydrographs were imposed on the system at the upstream face of the rockfills. The hydrographs were mainly different in terms of

Received on June 9, 2006. Accepted on September 23, 2006.

the rate of rise. Pressure transducers along the centerline of the flume bottom allowed the recording of the variable depth with time within the rockfill. This was done based on adoption of gradually-varied flow behavior for these structures. The experiments resulted in values of the hydraulic parameters of different media and created a set of data suitable for verifying any model that simulates unsteady flow through homogeneous and layered rockfills subject to an upstream hydrograph.

2 Background

Figure 1 is a schematic representation of flow through a hypothetical valley fill. Characteristics of this flow situation are identified here to clarify the physical behavior of the flow system. The characteristics aid the development of a mathematical formulation suitable for the physical system. The main characteristics of valley fills together with approaches selected to model these characteristics are described below.

(a) The media consists of coarse materials that make use of a non-linear flow law necessary.
(b) The valley fill structure is long compared to other man-made rockfill hydraulic structures. This implies that these structures have a high length-to-depth ratio compared to other rockfill structures (Fig. 1a). Therefore, a one-dimensional approach can be used to model the flow through the valley fill (Bari and Hansen, 2002; Greenly and Joy, 1996).
(c) Field studies on end-dumped valley fills show that the size of the material making up the valley fill changes significantly in the vertical direction due to natural segregation of the materials during dumping. This segregation results in a vertical variability of all material properties including the friction coefficients. This adds to the complexity of the flow system. This requires either a multiple dimensional approach to the modeling or a form of vertically averaging these properties.

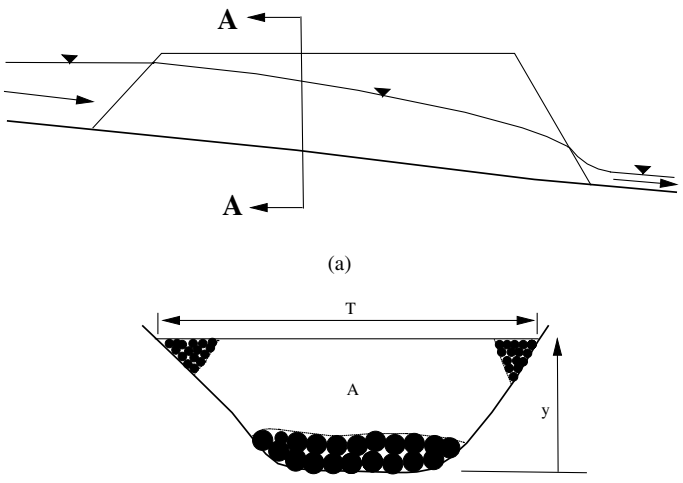

Figure 1 A valley fill configuration.

(d) Flow takes place in a valley with a non-rectangular and non-prismatic cross section. In ROCKFLOW, the generic shape considered for the valley is a trapezoidal shape (Fig. 1b). Side slopes of the valley can be different in either side of the cross section, and these, along with the base width can vary from section to section. This provides enough flexibility to reasonably approximate the shape of any valley cross section.

2.1 Non-linear flow analysis

Many different non-linear constitutive equations for steady flow through coarse porous media have been proposed in the literature. It has been shown theoretically (Ahmed and Sunada, 1969; Hassanizadeh and Gray, 1987; Irmay, 1958; Ma and Ruth, 1993) and statistically (Dullien, 1992; Joy, 1991) that the Forchheimer equation is, in general, superior to the other non-linear equations such as the power law equation. This equation includes a second velocity term to account for inertial terms in addition to the viscous effects represented by the Darcy equation. Therefore, the Forchheimer equation has been selected as the non-linear constitutive relationship of interest in ROCKFLOW. The Forchheimer equation has the following structure:

$$i = av + bv^2 \tag{1}$$

where i is the hydraulic gradient in the direction of flow, v is the bulk velocity of the flow, and a and b are media friction coefficients. Coefficients a and b depend on different properties of the media such as porosity, size, shape, and orientation of the particles.

Investigations show that unsteady flow through coarse porous media can be complicated from energy loss point of view, especially in flow through rubble-mound breakwaters under the effect of oscillatory waves. In these situations, the extended Forchheimer equation has been proposed as a substitute for the standard Forchheimer equation. This equation is basically the same equation originally proposed by Polubarinova-Kochina (1952):

$$i = av + bv^2 + C_a \frac{\partial v}{\partial t} \tag{2}$$

where t is time and C_a is a friction coefficient. As is discussed in section 5.2, the effect of the third term in Eq. (2) is negligible for flow through valley fills. This is due to the nature of the unsteady flow which is not a fast accelerating, oscillatory flow. Therefore, this additional term was not included in the model.

2.2 Equivalent friction coefficients

Figure 2 shows a general cross section of a valley fill with a heterogeneous rockfill in the vertical direction. Gradation of the materials in the vertical plane can be a continuous function of depth or can have sharp boundaries, depending on the method of placement of the material.

One approach to analyzing this system and properly representing the change in material properties is to use higher dimensional models. This has the advantage of properly representing the gradation but the disadvantage of requiring a two or

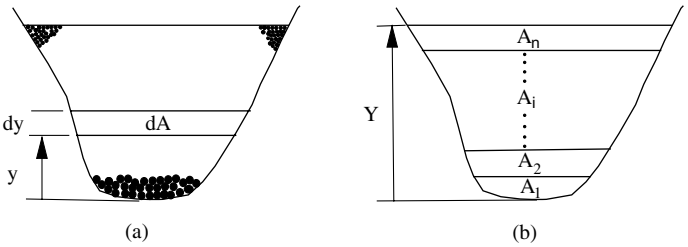

Figure 2 Geometry of a segregated valley fill.

three dimensional model which requires considerable computational effort and a large amount of data. The alternative is to consider a form of averaged media properties and analyzing the system as a one-dimensional problem. Hosseini and Joy (1997) analyzed the effect of segregation on flow behavior and found appropriate averaging schemes for the friction coefficients (a and b in the Forchheimer equation).

The objective of their approach was to represent the entire flow depth of the valley fill by single values of the friction coefficients a and b for cases where they clearly changed from level-to-level. In their approach, for any depth of flow Y consisting of n layers (as shown in Fig. 2), an equivalent hydraulic system is defined for which equivalent a and b values in the Forchheimer equation are found. Their approach is based on separating the losses into laminar and turbulent losses, finding equivalent a (a_{eq}) and equivalent$b$ (b_{eq}) separately and finally superposing the results to find the overall energy loss in the equivalent hydraulic system using:

$$i = a_{eq}V + b_{eq}V^2 \tag{3}$$

where a_{eq} and b_{eq} are the a and b coefficient for the equivalent hydraulic system and V is the average longitudinal bulk velocity.

The final result of their approach is to use Eq. (4) to find a_{eq} at any depth Y for a system that considers continuous variation of a with depth.

$$a_{eq} = \frac{A}{\int_0^Y \frac{dA}{a(y)}} \tag{4}$$

where A is the total cross sectional area at depth of flow Y, and $a(y)$ is a function that accounts for the variability of a with y. For the discretized configuration, necessary for numerical computation, shown in Fig. 2b, Eq. (4) for any flow depth can be written as:

$$a_{eq} = \frac{(A_1 + A_2 + \cdots + A_n)}{\left(\frac{A_1}{a_1} + \frac{A_2}{a_2} + \cdots + \frac{A_n}{a_n}\right)} = \frac{\sum A_i}{\sum\left(\frac{A_i}{a_i}\right)} \tag{5}$$

where A_i and a_i refer to the cross sectional area and the coefficient a in each subsection i, respectively.

In an analogous fashion, similar equations with similar notations are used to find b_{eq} as follows:

$$b_{eq} = \frac{A^2}{\left(\int_0^Y \frac{dA}{\sqrt{b(y)}}\right)^2} \tag{6}$$

$$b_{eq} = \frac{(A_1 + A_2 + \cdots + A_n)^2}{\left(\frac{A_1}{\sqrt{b_1}} + \frac{A_2}{\sqrt{b_2}} + \cdots \frac{A_n}{\sqrt{b_n}}\right)^2} \tag{7}$$

The derived Eqs. (5) and (7) are reported in terms of the cross sectional area rather than thickness. Therefore, the equations can be easily applied to valley fills with variable widths as long as the variability of the cross section with depth can be defined.

2.3 Governing equations

Use of the one-dimensional gradually varied flow equation is a common practice in the analysis of steady flow through rockfill structures (Bari and Hansen, 2002; Garga *et al.*, 1989; Leps, 1973; Parkin, 1991; Stephenson, 1979). The one-dimensional approach ignores changes in velocity in the vertical and lateral directions and assumes a hydrostatic pressure distribution. Although this has been applied to different rockfill structures, the approach is more acceptable for valley fills and rock drains (Greenly and Joy, 1996). This is due to the fact that these structures have a high length-to-depth ratio compared to the other structures.

To model unsteady flow through rockfill, the modified Saint-Venant equations were used. Modifications to these equations for flow through rockfill were obtained by applying the momentum equation to a control volume of flow. The results for a valley with a general cross-sectional shape are outlined below.

Momentum equation:

$$-A\frac{\partial y}{\partial x} + A(S_0 - S_f) = \frac{1}{n^2 g}\frac{\partial\left(\frac{Q^2}{A}\right)}{\partial x} + \frac{1}{ng}\frac{\partial Q}{\partial t} \tag{8}$$

Continuity equation:

$$\frac{\partial Q}{\partial x} = -n\frac{\partial A}{\partial t} \tag{9}$$

Constitutive relationship (Forchheimer Equation):

$$S_f = aV + bV^2 \tag{10}$$

where x is the longitudinal direction of flow, y is the depth of flow, t is time, A is the cross sectional area of flow, S_o is the bed slope of channel, S_f is the slope of the energy grade line, n is the porosity of media, g is the gravitational acceleration, Q is the volumetric discharge, V is the longitudinal bulk velocity, and a and b are coefficients in the Forchheimer equation.

Similar governing equations have also been developed by Stephenson (1979) for a rockfill with a rectangular cross section. For the sake of simplicity, here, Eqs (8) to (10) have been written for a homogeneous media. However, in section 3, in the process of development of the model, the methodology for including the varibility of material properties is presented.

The boundary conditions associated with Eqs (8) and (9) are:

Upstream Boundary Conditions:
An imposed hydrograph: $Q_{upstream} = Q(t)$
or
A recorded history of upstream depth: $y_{upstream} = y(t)$
Downstream Boundary Conditions:
A recorded history of downstream depth governed by some downstream conditions (e.g. a lake):

$$y_{downstream} = y(t)$$

or
The natural exit depth of the fill geometry and discharge, i.e. the critical-flow condition:

$$\frac{Q^2 T}{n^2 g A^3} = 1$$

where in the boundary conditions, $y(t)$ and $Q(t)$ values refer to the specified values of depth and discharge at the boundaries as a function of time.

A two-dimensional approach, which considers the curvature of streamlines in the vertical plane, also can be used to analyze unsteady flow. Samani *et al.* (2003) used this approach to conduct reservoir routing through rockfill dams. They defined a 2-D unsteady continuity equation and combined it with a non-linear constitutive relationship ignoring acceleration terms. Although the way that they have included storage term in their continuity equation needs further clarification, applying their method to heterogeneous valley fills adds more difficulty and inflexibility compared to accuracy which may be gained.

3 Model development

Model development requires three primary issues be addressed. Firstly, how to represent the system in an appropriate numerical manner. Secondly, because the problem is highly non-linear an appropriate iteration scheme needs to be applied to account for this non-linearity. Finally, since the exit is usually sloped the effective length of the structure is variable and this also needs to be included. The effective length is defined as the distance between exit point and beginning of the rockfill. These three issues are addressed below.

3.1 Numerical scheme

Except for a few trivial cases, the governing equations cannot be solved analytically. In this case a solution has been developed using an appropriate finite difference scheme together with the related initial and boundary conditions. The weighted four-point finite difference scheme (Fread, 1993; Singh, 1996) was used to solve the governing partial differential equations together with the initial and boundary conditions. The method was first used by Preissman in 1961 (Abbot and Basco, 1989).

In a domain discretized over distance and time, the method approximates any general function f and its derivatives as:

$$f = \theta\left(\frac{f_{i+1}^{j+1} + f_i^{j+1}}{2}\right) + (1-\theta)\left(\frac{f_{i+1}^{j} + f_i^{j}}{2}\right) \tag{11}$$

$$\frac{\partial f}{\partial t} = \frac{f_i^{j+1} - f_i^j + f_{i+1}^{j+1} - f_{i+1}^j}{2\Delta t} \tag{12}$$

$$\frac{\partial f}{\partial x} = \frac{\theta\left(f_{i+1}^{j+1} - f_i^{j+1}\right)}{\Delta x_i} + \frac{(1-\theta)\left(f_{i+1}^{j} - f_i^{j}\right)}{\Delta x_i} \tag{13}$$

where i and j refer to distance and time steps, respectively, and θ is a weighting factor that varies between 0 and 1. In order to apply the scheme to the governing partial differential equations, the momentum (Eq. (8)) and continuity (Eq. (9)) equations were rearranged as:

$$\frac{\partial y}{\partial x}\left(A - Fr^2 A\right) - A\left(S_o - S_f\right) + \frac{1}{ng}\frac{\partial Q}{\partial t} = 0 \tag{14}$$

$$\frac{\partial Q}{\partial x} + n\frac{\partial A}{\partial t} = 0 \tag{15}$$

where Fr is Froude number for flow through porous media defined as:

$$Fr = \left(\frac{Q^2 T}{n^2 g A^3}\right)^{\frac{1}{2}} \tag{16}$$

In the Froude Number, T is the top width of the flow as shown in Fig. 1b.

Applying the differencing schemes in Eqs. (11) to (13) to Eqs. (14) and (15) gives the following finite difference equations:

$$\left[\theta\left(\frac{y_{i+1}^{j+1} - y_i^{j+1}}{\Delta x_i}\right) + (1-\theta)\left(\frac{y_{i+1}^{j} - y_i^{j}}{\Delta x_i}\right)\right]\left(\bar{A} - \bar{Fr}^2\bar{A}\right) - \bar{A}\left(S_o - \bar{S}_f\right) + \frac{1}{\bar{n}g}\left(\frac{Q_{i+1}^{j+1} - Q_{i+1}^{j}}{2\Delta t} + \frac{Q_i^{j+1} - Q_i^{j}}{2\Delta t}\right) = 0 \tag{17}$$

$$\left[\theta\left(\frac{Q_{i+1}^{j+1} - Q_i^{j+1}}{\Delta x_i}\right) + (1-\theta)\left(\frac{Q_{i+1}^{j} - Q_i^{j}}{\Delta x_i}\right)\right] + \bar{n}\left(\frac{A_{i+1}^{j+1} - A_{i+1}^{j}}{2\Delta t} + \frac{A_i^{j+1} - A_i^{j}}{2\Delta t}\right) = 0 \tag{18}$$

with:

$$\bar{y} = \theta\left(\frac{y_{i+1}^{j+1} + y_i^{j+1}}{2}\right) + (1-\theta)\left(\frac{y_{i+1}^{j} + y_i^{j}}{2}\right)$$

$$\bar{Q} = \theta\left(\frac{Q_{i+1}^{j+1} + Q_i^{j+1}}{2}\right) + (1-\theta)\left(\frac{Q_{i+1}^{j} + Q_i^{j}}{2}\right)$$

$$\bar{Fr}^2 = \frac{\bar{Q}^2\bar{T}}{g\bar{A}^3\bar{n}^2}$$

$$\bar{S}_f = \bar{a}\bar{V} + \bar{b}\bar{V}^2$$

$$\bar{n} = n_{i+1/2}\,(\bar{y})$$

$$\bar{A} = A_{i+1/2}\,(\bar{y})$$

$$\bar{V} = \frac{\bar{Q}}{\bar{A}}$$

$$\bar{T} = T_{i+1/2}\,(\bar{y})$$

$$\bar{a} = a_{i+1/2,eq}\,(\bar{y})$$

$$\bar{b} = b_{i+1/2,eq}\,(\bar{y})$$

In the above, properties such as $A_{i+1/2}\,(\bar{y})$, which are calculated midway between 2 nodes, are based on the mean depth($\bar{y}$)and the mean of geometrical properties such as the bottom width between nodes i and $i+1$. The finite difference equations are highly non-linear due to the dependency of the coefficients on the unknown variables. Averaging material properties in the vertical plane also adds to the non-linearity of the system. Because of these non-linearities, the Newton-Raphson iterative scheme was used to solve the equations. The following discussion of this method is drawn from Chow *et al.* (1988) and Singh (1996) to describe the applied procedure.

In vector form, a system of non-linear equations of a vector of unknowns, $\vec{X}$, can be represented as:

$$\vec{f}\left(\vec{X}\right) = 0 \tag{19}$$

The solution of Eq. (19) by iteration is written as:

$$\vec{f}\left(\vec{X}^{k+1}\right) \approx \vec{f}\left(\vec{X}^{k}\right) + J\left(\vec{X}^{k}\right)\left(\Delta\vec{X}^{k}\right) \tag{20}$$

where k refers to the iteration number, $J\left(\vec{X}^{k}\right)$ is the Jacobian matrix consisting of the first derivatives of $\vec{f}\left(\vec{X}\right)$ calculated at $\vec{X}^{k}$ and $\Delta\vec{X}^{k}$ is the change required to improve the previous solution toward the correct solution. When the correct solution for the unknowns is arrived at, $\vec{f}\left(\vec{X}^{k+1}\right)$ in Eq. (20) is 0. Therefore:

$$J\left(\vec{X}^{k}\right)\left(\Delta\vec{X}^{k}\right) = -\vec{f}\left(\vec{X}^{k}\right) \tag{21}$$

The right hand side of Eq. (21) is the negative of the residual vector at iteration k. By solving the linear system of equations (Eq. (21)), the iteration improvement, $\Delta\vec{X}^{k}$, can be obtained considering that$J\left(\vec{X}^{k}\right)$ is a known coefficient matrix that is updated after each iteration. This procedure is repeated until all elements of $\Delta\vec{X}^{k}$ are smaller than some set of specified tolerances.

In Eqs (17) and (18), there are two unknowns at each node: depth and discharge. Thus for a system consisting of N nodes, there are $2N$ unknowns at time $j+1$. Therefore, the vector of unknowns at time $j+1$ is:

$$\vec{X} = (y_1, Q_1, \ldots, y_i, Q_i, \ldots, y_N, Q_N) \tag{22}$$

The continuity and momentum equations written for $N-1$ elements result in $2N-2$ equations. The other two equations required for solving the unknowns are obtained from the boundary conditions applied to the boundary nodes. The resulting equations can be written in the following format:

$$\begin{aligned}
UBE\,(y_1, Q_1) &= 0\\
CE_1\,(y_1, Q_1, y_2, Q_2) &= 0\\
ME_1\,(y_1, Q_1, y_2, Q_2) &= 0\\
&\vdots\\
CE_i\,(y_i, Q_i, y_{i+1}, Q_{i+1}) &= 0\\
ME_i\,(y_i, Q_i, y_{i+1}, Q_{i+1}) &= 0\\
&\vdots\\
CE_{N-1}\,(y_{N-1}, Q_{N-1}, y_N, Q_N) &= 0\\
ME_{N-1}\,(y_{N-1}, Q_{N-1}, y_N, Q_N) &= 0\\
DBE\,(y_N, Q_N) &= 0
\end{aligned} \tag{23}$$

In Eq. (23), *UBE* and *DBE* refer to the upstream and downstream boundary conditions, respectively, and *CE* and *ME* refer to the continuity and momentum equations, respectively. The initial estimate of $J\left(\vec{X}^{k}\right)$ to start the procedure was assumed to be the initial condition or the previous time solution.

The following equations were specifically derived and used in this study to find the derivative terms required to calculate the $J\left(\vec{X}^{k}\right)$:

$$\frac{\partial ME_i}{\partial y_i^{j+1}} = \frac{-\theta}{\Delta x_i}\bar{A}(1-\bar{F}r^2) + \frac{\partial \bar{A}}{\partial y_i^{j+1}}\left[\theta\left(\frac{y_{i+1}^{j+1}-y_i^{j+1}}{\Delta x_i}\right) + (1-\theta)\left(\frac{y_{i+1}^{j}-y_i^{j}}{\Delta x_i}\right)\right]$$

$$(1-\bar{F}r^2) - \frac{\partial \bar{A}}{\partial y_i^{j+1}}(S_o - \bar{S}_f) - \bar{A}\left(\frac{\bar{a}\bar{Q}}{\bar{A}^2} + \frac{2\bar{b}\bar{Q}^2}{\bar{A}^3}\right)\frac{\partial \bar{A}}{\partial y_i^{j+1}} \tag{24}$$

$$\frac{\partial ME_i}{\partial Q_i^{j+1}} = \frac{1}{2\bar{n}g\Delta t} + \bar{A}\theta\left(\frac{\bar{a}}{\bar{A}} + \frac{2\bar{b}}{\bar{A}^2}\bar{Q}\right) \tag{25}$$

$$\frac{\partial ME_i}{\partial y_{i+1}^{j+1}} = \frac{\theta}{\Delta x_i}\bar{A}(1-\bar{F}r^2) + \frac{\partial \bar{A}}{\partial y_{i+1}^{j+1}}\left[\theta\left(\frac{y_{i+1}^{j+1}-y_i^{j+1}}{\Delta x_i}\right) + (1-\theta)\left(\frac{y_{i+1}^{j}-y_i^{j}}{\Delta x_i}\right)\right]$$

$$\left(1-\bar{F}r^2\right) - \frac{\partial \bar{A}}{\partial y_{i+1}^{j+1}}(S_o - \bar{S}_f) - \bar{A}\left(\frac{\bar{a}\bar{Q}}{\bar{A}^2} + \frac{2\bar{b}\bar{Q}^2}{\bar{A}^3}\right)\frac{\partial \bar{A}}{\partial y_{i+1}^{j+1}} \tag{26}$$

$$\frac{\partial ME_i}{\partial Q_{i+1}^{j+1}} = \frac{1}{2\bar{n}g\Delta t} + \bar{A}\theta\left(\frac{\bar{a}}{\bar{A}} + \frac{2\bar{b}}{\bar{A}^2}\bar{Q}\right) \tag{27}$$

$$\frac{\partial CE_i}{\partial y_i^{j+1}} = \frac{\bar{n}T_i^{j+1}}{2\Delta t} \tag{28}$$

$$\frac{\partial CE_i}{\partial Q_i^{j+1}} = -\frac{\theta}{\Delta x_i} \tag{29}$$

$$\frac{\partial CE_i}{\partial y_{i+1}^{j+1}} = \frac{\bar{n}T_{i+1}^{j+1}}{2\Delta t} \tag{30}$$

$$\frac{\partial CE_i}{\partial Q_{i+1}^{j+1}} = \frac{\theta}{\Delta x_i} \tag{31}$$

The derivatives of the critical-flow boundary condition defined at node N and time $j+1$ are:

$$\frac{\partial DBE}{\partial y} = Q^2 \frac{\partial T}{\partial y} - 3gA^2n^2 \frac{\partial A}{\partial y} \tag{32}$$

$$\frac{\partial DBE}{\partial Q} = 2QT \tag{33}$$

The other boundary conditions introduced in section 2 are linear functions of Q and y and have a derivative of either 1 or 0. The $\frac{\partial A}{\partial y}$ and $\frac{\partial T}{\partial y}$ terms are easily related to the geometry of the cross section of the channel.

After developing the Jacobian matrix and the negative of the residual vector, the resulting linear system in Eq. (21) must be solved. The Choleski method for non-symmetric banded matrix in vector storage (Istok, 1989) was used to solve the equations.

3.2 Sloped downstream faces

The exit presents two problems in the analysis. Firstly, what is the exit depth if it is not determined by some downstream condition? Secondly, because the downstream face is sloped, the effective length of the structure will change with discharge. This is particularly true for the last element in the finite difference scheme described above.

Three methods or equations are found in the literature that introduce an exit depth for rockfill structures as a necessity to solve the gradually-varied flow equation inside the rockfill under steady-state conditions (Hansen, 1992). The depth calculated by these methods is applied provided that it exceeds the tailwater depth downstream of the rockfill. If not, the tailwater level provides the downstream control. Hansen (1992), based on extensive flume studies conducted on different rockfills, concluded that the critical depth approach proposed by Stephenson (Stephenson, 1978; 1979) works better than other methods. Therefore, this approach was selected as the method for calculation of the exit location.

In unsteady-state situations, the downstream depth varies with time because discharge varies with time. This means that the location that this depth meets with the downstream face changes with time. In order to deal with the variability of the downstream location, the co-ordinate of the last node must be adjusted at each time step (Fig. 3) using the following equation:

$$x_N^{j+1} = x_N(fixed) - \frac{y_N^j}{\tan(\beta)} \tag{34}$$

where x_N^{j+1} is the adjusted co-ordinate of node N at time step $j+1$, $x_N\,(fixed)$ is the fixed co-ordinate of the lower end of the rockfill, and β is the slope of downstream face. This methodology provides a means for imposing a variable downstream depth by varying the size of the last element. In order that the last element always be present in the process of calculations, the following restriction must also be satisfied:

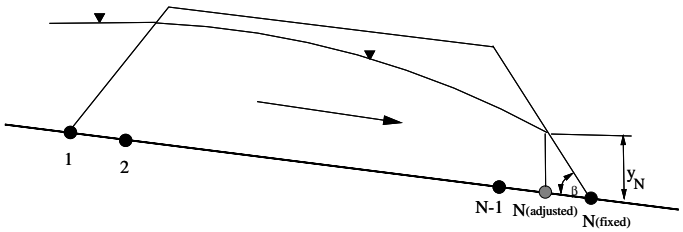

Figure 3 Location adjustment of the last node for rockfills with sloped downstream faces.

$$x_{N-1} < x_N(fixed) - \frac{y_{N,\max}}{\tan(\beta)} \tag{35}$$

where $y_{N,max}$ is an estimated maximum downstream depth. This estimation can be easily made by looking at the history of the downstream depth. If it is a critical-flow boundary condition, the estimate can be made by calculating the critical depth based on the peak of the imposed upstream hydrograph considering that the flood wave attenuates as it leaves the rockfill.

4 Experimental setup and data

4.1 Media physical properties

Three types of materials selected in this study were different in size ranging from 8.7 mm to 25.7 mm. Although each material had been mechanically sorted in the quarry, it was washed and completely mixed in the laboratory to produce a media as uniform as possible. Three samples were randomly drawn from each material. Each sample was about 25 kg. For each sample the size distribution, particle density, porosity and shape factor were determined using standard methods. Shape factors (SF) were estimated using the following relationship:

$$SF = \frac{c^*}{\sqrt{a^*b^*}} \tag{36}$$

where a^* is length in longest direction and b^* are c^* are lengths measured in mutually perpendicular medium and short directions, respectively.

The average of these physical parameters for the three samples was considered to be the average for the material. Table 1 summarizes the results.

4.2 Flume tests

Fig. 4 shows the details of the flume used. It was modified for the free-surface flow experiments, by placing a tank in the beginning of the flume to create hydrographs with different shapes.

As shown in Fig. 4, the 60.3 cm wide flume was made of plywood except for the glass side to view the flow pattern. The elevation of the bottom of the flume was measured at different pressure transducer locations by a leveling procedure accurate to 1.0 mm. The overall bed slope was found to be 0.0058. A movable

Table 1 Material properties.

Material	d_{50} (mm)	d_{10} (mm)	Coef. of uniformity (−)	Coef. of concavity (−)	Particle density (g/cm^3)	Porosity (−)	Shape factor (−)
Small	8.6	5.6	1.61	1.05	2.75	0.483	0.47
Medium	21.1	15.1	1.45	1.13	2.71	0.458	0.53
Large	26.9	20.4	1.38	1.02	2.60	0.443	0.50

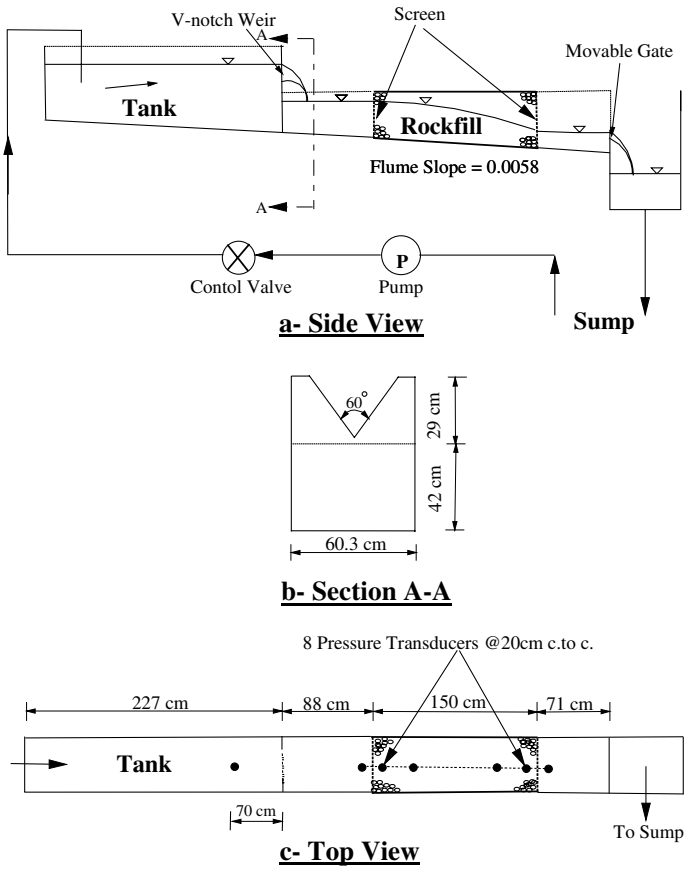

Figure 4 Plexiglas flume and experimental set-up.

gate at the end of the flume was used to control the downstream water level.

A 150 kW self priming centrifugal pump, was used to deliver water to the system. The water first passed through the upstream tank which was made of plywood with the key dimensions shown in Fig. 4. A V-notch weir installed at the outlet of the tank was used to measure the discharge rate supplied to the rockfill.

Three of the rockfill structures were 150.0 cm long, 60.3 cm wide, and 40.0 cm high and made of three different materials as described in section 4.1. The fourth rockfill was a layered system of the same length and width with the largest material in the bottom and the smallest material at the top. The thickness of the large material in the bottom was 12.0 cm while those of the others were 12.0 and 16.0 cm for the medium and small materials, respectively. All rockfills were constructed under a loose (uncompacted) condition. Two rigid screens with openings appropriate to contain the large and medium materials were used upstream and downstream of the rockfill to create vertical faces for the rockfill structures. In the case of the small material, a 6.3 × 6.3 cm wire mesh was also used. The head loss through the screen system was determined to be negligible.

Ten (0−1.45 psi) pressure transducers were used to record the unsteady flow behavior inside the rockfill. One pressure sensor was installed 5.0 cm upstream of the rockfill to record the upstream depth with time and one 5.0 cm downstream to record the downstream depth. Eight pressure transducers were installed every 20.0 cm inside the rockfill. Two of these eight pressure sensors were located 5.0 cm inside the rockfill at both ends. All pressure sensors were connected to manometers installed on a manometer board and linked to a Campbell Scientific CR10 datalogger. The exact locations of the pressure sensors were outside, near the bottom of the flume. They were connected to the flow at the bottom using copper tubings. However, the datum for head measurements was considered to be the inner part of the bottom of the flume.

One pressure transducer was also installed 70.0 cm upstream of the weir to record the rate of rise or fall of water behind the weir. The weir was a 60°V-notch weir made of stainless steel with a thickness of 2 mm. The calibrated relationship between the head upstream of this weir and discharge, with a $R^2 = 0.998$ in the range of the experimental discharges, defined the pattern of the imposed hydrograph.

The experimental procedure used in the flume tests can be described under two different headings, steady and unsteady state conditions, for each rockfill.

4.2.1 Steady-state conditions

The pump was used to deliver water to the system with a constant discharge. Steady state was determined after the head behind the V-notch weir had reached a constant level. When the steady-state condition was stabilized, all manometer readings in the system were recorded. The exit depth at the downstream face of the rockfill was also measured using a fixed scale accurate to 1 mm under either free-flow conditions or drowned (controlled) conditions. Free-flow condition refers to the condition when a seepage face appears in the downstream face of the rockfill while the drowned condition is the situation where the gate at the end of flume was raised to create a drowned flow condition in the downstream face. Table 2 presents a summary of the different steady-state tests on the rockfills. In the table, almost free is the condition when the two conditions are not distinguishable.

Table 2 Steady-state test conditions.

Material	Discharge (L/s)	Upstream depth (mm)	Downstream condition	Measured exit depth (mm)	Water Temperature (°C)	Test name
Small (S)						
(1)	1.01	143	≅ Free	11	19.7	SS1
(2)	2.53	250	Controlled	63	19.7	SS2
(3)	3.97	330	Controlled	89	19.7	SS3
(4)	1.08	144	≅ Free	12	19.7	SS4
(5)	2.65	252	Controlled	62	19.7	SS5
(6)	4.11	334	Controlled	89	19.7	SS6
Medium (M)						
(1)	0.93	107	Controlled	30	19.8	MS1
(2)	2.78	213	Controlled	53	19.8	MS2
(3)	5.56	330	Controlled	76	19.8	MS3
(4)	1.00	107	Controlled	16	19.8	MS4
(5)	2.89	213	Controlled	39	19.8	MS5
(6)	5.62	327	Controlled	78	19.8	MS6
Large (L)						
(1)	2.89	191	Controlled	81	20.5	LS1
(2)	3.84	228	Controlled	84	20.5	LS2
(3)	7.67	353	Controlled	97	20.5	LS3
(4)	1.18	102	Controlled	19	20.5	LS4
(5)	3.43	204	Controlled	37	20.5	LS5
(6)	7.09	329	Controlled	69	20.5	LS6
Layered Rockfill (N)						
(1)	2.39	184	Free	24	20.5	NS1
(2)	3.93	261	≅ Free	54	20.5	NS2
(3)	6.31	380	Controlled	110	20.5	NS3
(4)	1.20	117	≅ Free	19	20.5	NS4
(5)	3.49	239	Free	41	20.5	NS5
(6)	5.71	342	Free	59	20.5	NS6

4.2.2 Unsteady-state conditions

The procedure for unsteady-state conditions was basically the same as that for steady-state conditions except for the fact that the discharge through the rockfill was varied. To accomplish this, the pump was started and set to a constant rate with the upstream tank initially empty. The rate of rise of water in the tank was recorded every second. Only once the water level reached the vertex of the V-notch weir did water enter the rockfill. This was considered as the starting time of the inflow hydrograph. The water level continued to increase in the head tank and hence the rising limb of hydrograph was created. The falling limb of the hydrograph was created by turning off the pump at a specific time. This time was considered the time that the reservoir behind the rockfill was nearly full indicating that the whole body of the rockfill at the upstream face was active in passing water.

The pressure transducers were recording the flow depths in the system every second during the rising and falling limbs. The rate of rise of the hydrograph was changed by adjusting the pump control valve. Three different hydrographs with three different rates of rise were created for each of the four rockfill structures in the flume.

Initial condition was a zero depth in the rockfill and the downstream condition was a free-flow situation for all hydrographs. Additional flow situations were also created by establishing a non-zero depth as an initial condition in the system. This was done by beginning with a constant discharge through the system and adjusting the heads using the movable gate at the end of the flume. This discharge and the resulting depths were recorded as the initial condition. The hydrograph was then created by increasing the discharge and turning off the pump or lowering the discharge using the control valve in the pump. The downstream faces of the rockfills were in a drowned-flow condition in these cases. The second kind of hydrograph was not created for the rockfill made of the medium material because it was the first material placed in the flume and this idea was not considered in the beginning of the experiments.

Table 3 shows the characteristics of the unsteady-state tests. Temperature values were the same as those reported in Table 2 for each material. For hydrographs that were flat near the peak for a period of time, time to peak was assumed to be the central value of that constant discharge period.

Different rates of rise were tested over the range from 0.10 to 0.68 (L/s)/s. From the results summarized in the table, it is noted

Table 3 Unsteady-state test conditions.

Material	Peak flow (L/s)	Time to peak (s)	Rate of rise ((L/s)/s)	Downstream condition	Maximum measured exit depth (mm)	Maximum measured upstream depth (mm)	Test name
Small (S)							
(1)	7.86	46.5	0.17	Controlled	81	382	SU1
(2)	11.86	19.0	0.62	Controlled	78	336	SU2
(3)	17.66	26.0	0.68	Free	–	394	SU3
(4)	13.55	35.0	0.39	Free	–	386	SU4
(5)	8.19	60.5	0.13	Free	–	371	SU5
Medium (M)							
(1)	12.99	37.5	0.35	Free	–	373	MU1
(2)	17.37	27.0	0.64	Free	–	369	MU2
(3)	7.87	63.0	0.12	Free	–	329	MU3
Large (L)							
(1)	7.53	76.0	0.10	Controlled	101	350	LU1
(2)	13.56	27.5	0.49	Controlled	101	358	LU2
(3)	13.56	39.0	0.35	Free	–	356	LU3
(4)	8.05	77.0	0.10	Free	–	346	LU4
(5)	18.07	28.5	0.63	Free	–	380	LU5
Layered Rockflll (N)							
(1)	7.89	54.0	0.15	Controlled	113	376	NU1
(2)	13.07	29.0	0.45	Controlled	115	397	NU2
(3)	13.22	36.0	0.37	Free	–	368	NU3
(4)	7.99	66.5	0.12	Free	–	352	NU4
(5)	16.25	24.0	0.68	Free	–	333	NU5

that, in general, a higher rate of rise corresponds to a smaller time to peak. Detailed measurements of the unsteady-state scenarios together with the ability of the model to predict such scenarios are discussed in section 5.2.

5 Evaluation of the model performance

The collected data can be considered as bench mark data to evaluate the performance of the ROCKFLOW model. The three standard steps i.e. code verification, parameter estimation and model verification (Anderson *et al.*, 1993) were followed to achieve this. The developed code for steady-state situations was verified using an example for which analytical solution was available. In this example, flow through a homogeneous rectangular (vertical upstream and downstream faces) valley fill of unit width was considered. The flow characteristics and the selected material properties are as follows:

q (discharge per unit width) $= 0.5\,\mathrm{m^2/s}$, n (porosity) $= 0.443$, $a = 0.82\,\mathrm{s/m}$, $b = 39.1\,\mathrm{s^2/m^2}$, $S_o = 0.0$ and L = Length of Rockfill $= 10.0\,\mathrm{m}$

It was assumed that the tailwater depth is small compared to the critical depth. Therefore, critical-flow condition gave an exit depth of 0.506 m. Steady gradually-varied flow equation has an analytical solution of the following form for the situation described (Hansen, 1992):

$$x = \left[\frac{by}{a^2} - \frac{y^2}{2qa} + \frac{\ln(y)}{gn^2b} - \frac{b^2q\ln(ay+bq)}{a^3} - \frac{\ln(ay+bq)}{gn^2b}\right]_{y_0}^{y_x} \tag{37}$$

where x is the distance y_x is from y_o (m).

For modeling purposes 11 nodes with equal, 1 m, spacing were used. The closure criterion was 0.00001 m. Fig. 5 compares the result of the numerical study with that of the analytical solution. As demonstrated by the figure, the model predicts the flow behavior inside the rockfill well. However, increasing the number of nodes results in better agreement between the model and the analytical solution especially close to the seepage face, a zone with high hydraulic gradients.

In order to partially verify the unsteady code developed, it was applied to steady-state example. All characteristics were the same as values reported except for the imposed upstream discharge. The upstream discharge in this case was a hydrograph. The discharge starts from 0 and varies linearly for 300 s up to a value of $0.5\,\mathrm{m^3/s}$. Then, the discharge was kept constant until the end of the simulation at 3000 s. As was expected, the unsteady-state model gave final depths exactly the same as the corresponding steady-state values.

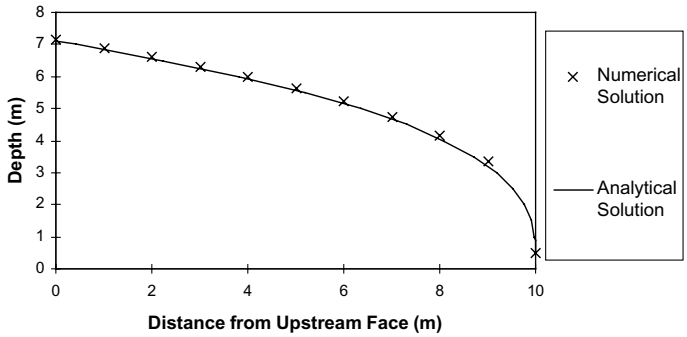

Figure 5 Steady-sate code verification-example.

5.1 Parameter estimation (Calibration)

The estimation of hydraulic parameters is a problem for rockfill structures. This is due to the fact that these lumped parameters are representative of spatially-variable physical properties of the media such as size and size distribution of the materials, porosity, orientation, shape and roughness of the particles. Local and the resulting average hydraulic effects of these properties are hard to quantify and therefore uncertainty will be an inherent ingredient of the estimated parameters.

In this study, the material hydraulic parameters were determined using steady-state runs in the model. The resulting hydraulic parameters were then used to model unsteady conditions. To achieve this, calibration techniques to determine in-situ hydraulic parameters were explored. Although the detailed presentation of these methods is beyond the scope of this paper, it is worth mentioning that the linear regression method suggested by Goodwill and Kalliontzis (1988) and non-linear regression using PEST software (Doherty *et al.*, 1994) were used. In general it was found that the values obtained using the PEST software performed the best both in terms of the overall behavior of the simulated water surface profiles and the upstream depth. Therefore the idea behind using PEST and the results obtained are briefly discussed here.

PEST, a model independent parameter estimation software tool (Doherty *et al.*, 1994) is a model that employs a non-linear estimation technique known as the Gauss-Marquardt-Levenberg method to find the best parameters in a weighted least-squares sense. The method can be applied to different discharge conditions of interest and the resulting parameters can be averaged. However, in this study, a simple modification was applied to the developed model to be able to calibrate for all steady-state conditions simultaneously. This modification was to create one input file containing all data related to the different conditions and have the model analyze this data in one run. As a result, one output file was developed and this made it possible for PEST to calibrate for all conditions simultaneously. The results obtained from this procedure are reported in Table 4. These are the results obtained from the simultaneous calibration of all tests for each material. In addition, the regression was done on the heads, and thus 48 data points were used to estimate the two parameters for each material. This provides enough degrees of freedom for making an estimate. The data points were given equal weight in the analysis. The results for layered rockfill were slightly different due to change in packing.

Table 4 Hydraulic parameters resulting from using PEST software.

Material	a (s/m)	95% Confidence interval a	b (s^2/m^2)	95% Confidence interval b
Small	2.73	±0.29	85.7	±11.1
Medium	1.79	±0.30	46.4	±7.9
Large	1.01	±0.17	39.7	±3.7

The results of applying PEST estimated parameters to flume rockfills show that the overall average absolute error in the upstream depth is less than 1%, and none greater than 6%.

5.2 Model verification

In order to verify the unsteady-state ROCKFLOW model, the unsteady-state tests summarized in Table 3 were used as independent data for the verification procedure. In this regard, the hydraulic parameters applicable to the rockfill materials were considered to be the in-situ parameters resulting from the calibration under steady-state conditions.

As was shown in Fig. 4, there is a reservoir between the rockfill and the weir where the hydrograph is measured. The role of this reservoir is important in flow behavior under unsteady-state conditions because it stores a relatively large volume of water. This zone was also included in the modeling by considering it as a zone with negligible energy loss compared to the rockfill and that a nearly horizontal water surface was observed in this zone during unsteady-state experiments. The a and b friction coefficients in the Forchheimer equation were assumed to be 0 for this zone. Small values of a and b such as 0.0001 s/m and 0.0001 s^2/m^2 that do not produce a difference in head along this storage area could be also considered.

To model the unsteady-state conditions, the model parameters selected were: $\Delta t = 1\,\text{s}$, $\Delta x = 0.1\,\text{m}$ and $\theta = 0.55$. Also, the depth and discharge tolerances were 10^{-4} m and 10^{-5} m^3/s, respectively. The selected parameter values provided sufficient accuracy for modeling. In general, the selected Δt and Δx values are compatible with the experimental measurements. At three locations, Δx values of 0.05 m, 0.05 m and 0.08 m were used to adapt the model to the geometry of the flume and measurement points.

To asses the effect of the third term in Eq. 2, assuming constant a and b for each material, it was found that for the conditions in the experimental apparatus, a maximum value of approximately 0.8 was appropriate for C_a (Hannoura and McCorquodale, 1985; Irmay, 1958; van Gent, 1995). It was included in the model and used in modeling flow through medium material. Examination of the water surface profiles at different times showed that the effect of this additional term was negligible (maximum change in calculated water depth of only 1 mm). Because of this small effect, this additional term was not included in the model.

Table 5 Measured and simulated peak characteristics of depth variation with time curves

Test name	Peak depth (time to peak) at upstream face			Peak depth (time to peak) at $x = 0.65$ m		
	Measured mm-(s)	Simulated mm-(s)	Difference (%)	Measured mm-(s)	Simulated mm-(s)	Difference (%)
SU1	382 (57)	376 (57)	−1.6 (0.0)	304 (60)	301 (61)	−1.0(1.7)
SU2	336 (31)	332 (30.5)	−1.2 (−1.6)	268(35)	265 (35.5)	−1.1(1.4)
SU3	394 (34)	380 (34.5)	−3.5 (1.5)	306 (39)	299 (40.5)	−2.3 (3.8)
SU4	386 (43)	379 (43)	−1.8 (0.0)	303 (47)	299 (48)	−1.3 (2.1)
SU5	371 (73)	367 (71)	−1.1 (−2.7)	293(74.5)	293(75)	0.0(0.7)
MU1	373 (44)	355 (43.5)	−4.8(1.1)	298 (46)	283 (47)	−5.3 (2.2)
MU2	369(34.5)	353(34)	−4.3 (−1.4)	296(37)	281 (37.5)	−5.1 (1.4)
MU3	329 (70.5)	324 (72.5)	−1.5 (2.8)	266 (73)	248 (75.5)	−6.8 (3.4)
LU1	350 (82)	327(80.5)	−6.6 (−1.8)	288(82)	269(82.5)	−6.6 (0.6)
LU2	358 (32)	355 (33.5)	−0.8 (4.7)	292 (36)	290 (35.5)	−0.7 (−1.4)
LU3	356 (43)	348 (42.5)	−2.2 (−1.2)	285 (44)	281 (44.5)	−1.4 (1.1)
LU4	347 (99)	348 (105.5)	0.3 (6.6)	282 (104)	284 (107)	0.7 (2.9)
LU5	379 (34)	373 (34)	−1.6 (0.0)	306 (35)	302 (37)	−1.3 (5.7)
NU1	376 (64)	370 (64)	−1.6 (0.0)	295 (66)	290(66.5)	−1.7(0.8)
NU2	396 (35)	390 (35.5)	−1.5 (1.4)	310 (37)	304 (38)	1.9 (2.7)
NU3	368 (42)	355 (43)	−3.5 (2.4)	282 (46)	272 (47)	−3.5 (2.2)
NU4	352 (76)	347 (76.5)	−1.4 (0.6)	272 (79)	268 (79)	−1.5 (0.0)
NU5	333 (31)	317 (33)	−4.8 (6.4)	256 (36)	243 (37)	−5.1 (2.8)

Figure 6 is a typical graphical presentation of the performance of the model under the reported unsteady-state conditions. These figures, drawn for all unsteady-state tests show the input hydrograph, water surface profiles at three representative times during the test and the depth variation with time at two representative locations.

A constant simulation time of 250 seconds was selected for all scenarios. This time was considered to be a sufficient time to study the overall behavior of the flow system in different zones such as the rising limb, peak zone and the falling limb of the depth variation with time curves. Table 5 summarizes the results in terms of some important flow characteristics such as maximum depth and time to maximum depth at two locations, the upstream face and at $x = 0.65$ m. Regarding the experimental and simulation results partially given in Table 5 and illustrated in Fig. 6 as a typical figure, the points reported below are observed and worth discussing.

(1) The depth results are good both in terms of the characteristics at the peak and overall performance of the depth variation with time curves considered at two locations, the upstream face and at $x = 0.65$ m. The average absolute difference between the simulated and the measured peak upstream depths is 2.5%, ranging from 0.3% to −6.6% while that of $x = 0.65$ m is 2.6% ranging from 0.0% to −6.8%.

(2) As shown in Table 5, a trend of underestimation of depth by the model is observed. However, such performance cannot be totally attributed to the model. The reason is that the flow of water entering the small reservoir upstream of the weir is not smooth. The impact of the accelerating jet of water running through the weir and entering the reservoir upstream the rockfill may cause an increase in depth that may propagate some distance downstream. The numerical model has not been developed to consider such secondary effects present in this complicated unsteady-state phenomena.

(3) The time results are also promising. On average, a difference of about 1.1 s is observed between the measured and simulated times. This difference is compatible with the accuracy in time measurements. The high difference in the case of LU4 test is due to relatively flat input hydrograph existed in this case.

(4) No major differences are observed between the performances of the model for different media.

(5) The curves predicted by the model follow the same pattern as the measured curves under different types of boundary and initial conditions. This is observed for both the depth variation with time and water surface profile curves. This also confirms that considering a critical flow in the downstream face of the rockfill under free-flow conditions leads to satisfactory results for unsteady-state conditions.

(6) Although some discrepancy is observed between the measured and simulated depths in the early stages of the flow, especially under non-zero depth initial conditions or rapidly rising hydrographs, the model is able to predict the more straight or concave-upward water surface profiles reasonably well.

(7) A concave-upward pattern was observed in water-surface profiles at early stages of the flow for all tests conducted under free-flow conditions. This is because it takes time for the flow to be affected by the downstream boundary condition and move towards the development of a fully-developed, concave-downward water surface profile. This time gets smaller as the material gets larger under the same imposed hydrograph.

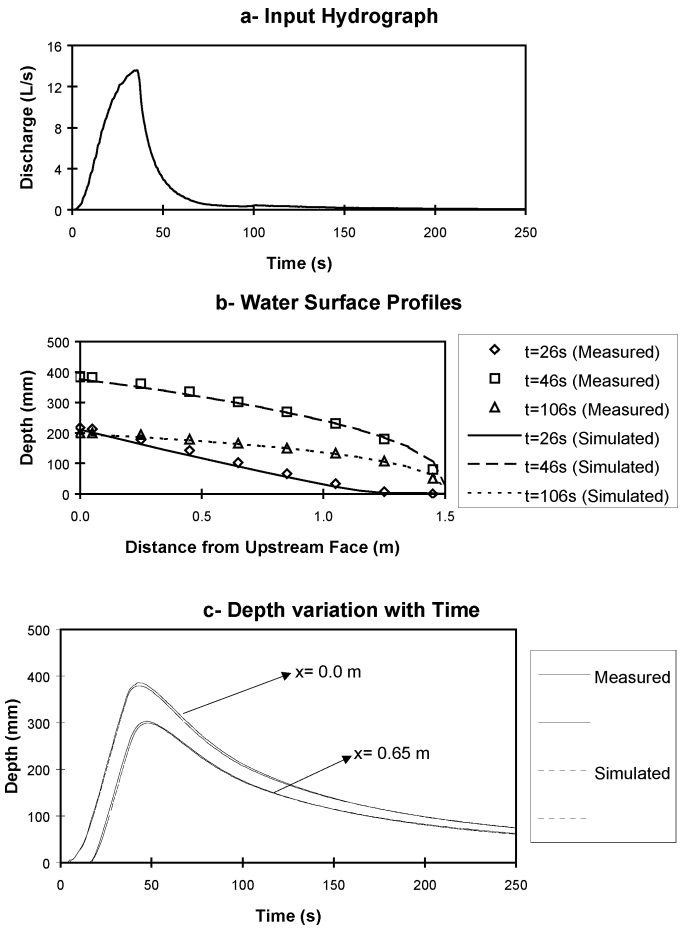

Figure 6 Unsteady-state model verification- SU4 test.

Considering the uncertainty and secondary effects present in physical modeling of unsteady flow through rockfill as a media susceptible to disturbance, and also the above discussed points, it can be concluded that the model has produced good results. Also, the fact that model was tested under variety of materials, and initial and boundary conditions, supports the potential for the applicability of the model to field conditions.

6 Conclusions

An unsteady model, ROCKFLOW, with a potential to use in the analysis of non-linear flow through heterogeneous valley fills was developed. It was concluded that the model works well based on the following evidence:

(a) The code verification of the model was successful,
(b) The model was able to simulate the experimental results well in terms of peak characteristics of depth variation with time curves at two representative locations, the upstream face and at $x = 0.65$ m as reported in Table 5,
(c) The overall pattern of modelled depth variation with time curves and water surface profiles was the same as the experimental results for different types of initial and boundary conditions, and
(d) No major differences were found between the performance of the model under different media, homogeneous or layered.

The following points were also concluded from the modeling exercises:

(e) A critical-flow condition at the downstream face of the rockfill under free-flow conditions was found to work well under unsteady-state conditions, and
(f) Times to peak of the depth variation with time curves were less sensitive to the choice of the model parameters compared to the depth itself.

As a final point, it can be concluded that the developed model has the potential for application to field situations considering its structure, capabilities, and performance briefly reviewed in the paper. The choice of the model parameters and the methods of the estimation of the hydraulic parameters will also help engineers to precisely model such a phenomenon.

Notations

A	total area of the cross section at any depth (m^2)
a	parameter in the Forchheimer equation (s/m)
a_{eq}	value of a in the Forchheimer equation for an equivalent hydraulic system (s/m)
a^*	length in longest direction of a particle
b	parameter in the Forchheimer equation (s^2/m^2)
b_{eq}	value of b in the Forchheimer equation for an equivalent hydraulic system (s^2/m^2)
C_a	parameter in the extended Forchheimer equation (s^2/m)
b^*, c^*	lengths measured in mutually perpendicular medium and short directions of a particle, respectively
CE	continuity equation
DBE	downstream boundary condition equation
f	general function
Fr	Froude number
g	gravitational acceleration (m/s^2)
i	hydraulic gradient
i	subscript referring to the nodes in longitudinal direction
j	superscript referring to time step
k	superscript indicating iteration number
L	total length of rockfill (m)
ME	momentum equation
n	porosity
N	number of nodes in finite difference discretization
Q	discharge (m^3/s)
SF	shape factor
S_o	bed slope
S_f	slope of energy grade line
t	time (s)
T	top width (m)
UBE	upstream boundary condition equation
v	bulk velocity of flow (m/s)
V	average longitudinal bulk velocity of flow (m/s)
x	longitudinal direction
$\vec{X}$	vector of unknowns
y	depth of flow (m)
Y	total depth of flow for a layered system (m)

$y_{N,max}$	estimated maximum downstream depth (m)
β	slope of downstream face of the rockfill
θ	weighting parameter in weighted four-point finite difference formulation
Δt	time step (s)
Δx	distance step (m)

References

1. ABBOTT, M.B. and BASCO, D.R. (1989). *Computational Fluid Dynamics*: *An Introduction for Engineers*, Longman Scientific & Technical, Longman Group UK Limited.
2. AHMED, N. and SUNADA, D.K. (1969). "Nonlinear Flow in Porous Media," *J. Hydr. Div.,* ASCE, 91(HY6), 1847–1857.
3. ANDERSON, M.P., WARD, D.S., LAPPALA, E.G. and PRICKETT, T.A. (1993). Computer Models for Subsurface Water, in D.R. Maidment (ed.), *Handbook of Hydrology*, McGraw-Hill, NY.
4. AUBERTIN, M., BRUNO, B. and CHAPUIS, R.P. (1996). "Hydraulic Conductivity of Homogonized Tailings from Hard Rock Mines," *Can. Geotech. J.*, 33, 470–482.
5. BARI, R. and HANSEN, D. (2002). "Application of Grdually-Varied flow Algorithms to Simulate Buried Streams," *J. Hydr. Res.*, IAHR, 40(6), 673–683.
6. CHOW, V.T., MAIDMENT, D.R. and MAYS, L.W. (1988). *Applied Hydrology*, McGraw-Hill, NY.
7. COWHERD, D.C. (1981). Hydrologic Consequences, Sediment Control, and Concurrent Reclamation of Dumped Valley Fills, in *Symp. on Surface Min. Hydrol., Sedimentol. and Recl.*, University of Kentucky, pp. 409–415.
8. DOHERTY J., BREBBER, L. and WHYTE P. (1994). PEST, Model Independent Parameter Estimation User's Manual, Watermark Computing.
9. DULLIEN, F.A.L. (1992). *Porous Media*: *Fluid Transport and Pore Structure*, Academic Press, U.S.A.
10. FINDIKAKIS, A.N. and TU, S-W. (1985). Flood Routing through Rock Dumps in Natural Channels, *Proc. of Conf. on Hydr. and Hydrol. in Small Comput. Age*, ASCE, Lake Buena Vista, Florida, pp. 1213–1218.
11. FREAD, D.L. (1993). Flow Routing, in D.R. Maidment (ed.), *Handbook of Hydrology*, McGraw-Hill, NY.
12. GARGA, V.K., HANSEN, D. and TOWNSEND, D.R. (1989). Considerations in the Design of Flow Through Rockfill Drains, *14th Mine Recl. Symp.*, Min. Assoc. of B.C., Cranbrook, British Columbia.
13. GOODWILL, I.M. and KALLIONTZIS, C. (1988). "Identification of Non-Darcy Groundwater Flow Parameters," *Int. J. Numer. Methods Fluids*, 8, 151–164.
14. GREENLY, B.T. and JOY, D.M. (1996). "One-Dimensional Finite Element Model for High Flow Velocities in Porous Media," *J. Geotech. Engrg.*, ASCE, 122(10), 789–796.
15. HANNOURA, A. and MCCORQUODALE, J.A. (1985). Rubble Mounds: Hydraulic Conductivity Equation," *J. Waterw., Port, Coast and Ocean Div,* ASCE, 111(4), 783–799.
16. HANSEN, D. (1992). The Behaviour of Flowthrough Rockfill Dams, Ph.D. Thesis, Department of Civ. Engrg, Univ. of Ottawa, Ottawa, Ontario, Canada.
17. HASSANIZADEH, S.M. and GRAY, W.G. (1987). "High Velocity Flow in Porous Media," *Transp. Porous Media,* 2, 521–531.
18. HOSSEINI, S.M. and JOY, D.M. (1997). Equivalent Friction Coefficients for Non-linear Flow through Heterogeneous Porous Media, *Proceedings of the 25th CSCE Annual Conference*, Sherbrooke, Quebec, Vol. 5, pp. 197–202.
19. IRMAY, S. (1958). "On the Theoretical Derivation of Darcy and Forchheimer Formulas," *Trans. of Am. Geophys. Union*, 39(4), 702–707.
20. ISTOK, J. (1989). *Groundwater Modelling by the Finite Element Method*, American Geophysical Union: Water Resources Monograph 13.
21. JOY, D.M. (1990). Sediment Transport Through Valley Fills, Paper presented at the Ann. GAC-MAC Conf., Vancouver, British Columbia.
22. JOY, D.M. (1991). Non-linear Flow in a Coarse Porous Media, *Proc. of the 1991 Ann. Conf. of CSCE*, Vol. 1, Vancouver, British Columbia, pp. 106–115.
23. LEPS, T.M. (1973) Flow through Rockfill, in Hirchfeld R. and Poulos S. (eds.), *Embankment Dam Engineering*, John-Wiley & Sons, NY.
24. MA, H. and RUTH, D.W. (1993). "The Microscopic Analysis of High Forchheimer Number Flow in Porous Media," *Transp. Porous Media*, 13, 139–160.
25. PARKIN, A.K. (1991). Through and Overflow Rockfill Dams, in E. Maranha das Neves (ed.), *Advances in Rockfill Structures*, Kluver Academic Publishers, The Netherlands, pp. 571–592.
26. POLUOBARINOVA-KOCHINA, Ya.P. (1952). *Theory of Groundwater Movement* (in Russian), English Translation by R.M.J. DeWiest, Princeton University Press, Princeton, N.J.
27. SAMANI H.M.V., SAMANI, J.M.V. and SHAIANNEJAD, M. (2003). "Reservoir Routing using Steady and Unsteady Flow through Rockfill Dams," *J. Hydr. Engrg.*, ASCE, 129(6), 448–454.
28. SINGH, V.P. (1996). *Kinematic Wave Modeling in Water Resources: Surface-Water Hydrology*, John-Wiley & Sons, NY.
29. STEPHENSON, D. (1978). Hydraulics of Gabions and Rockfill, *Proc. of XVI Convegno di Idraulica e Costruzioni Idrauliche*, Torino, Italy, pp. B31-1–B31-11.
30. STEPHENSON, D. (1979). Rockfill in Hydraulic Engineering, Developments in Geotechnical Engineering 27, Elsevier Scientific Publishing Co., Amsterdam, The Netherlands.
31. VAN GENT, M.R.A. (1995). "Porous Flow through Rubble-Mound Material," *J. Waterw., Port, Coast and Ocean Engrg.,* ASCE, 121(3), 176–181.